Proteomic analyses of ECM during pancreatic ductal adenocarcinoma progression reveal different contributions by tumor and stromal cells

Proteomic analyses of ECM during pancreatic ductal adenocarcinoma progression reveal different contributions by tumor and stromal cells

Chenxi Tian[a], Karl R. Clauser[b,1], Daniel Öhlund[c,d,e,1], Steffen Rickelt[a], Ying Huang[a], Mala Gupta[f], D. R. Mani[b], Steven A. Carr[b], David A. Tuveson[c], and Richard O. Hynes[a,g,2]

[a]Koch Institute for Integrative Cancer Research, Massachusetts Institute of Technology, Cambridge, MA 02139; [b]Broad Institute of MIT and Harvard, Cambridge, MA 02142; [c]Cold Spring Harbor Laboratory, Cold Spring Harbor, NY 11724; [d]Department of Radiation Sciences, Umeå University, 901 87 Umeå, Sweden; [e]Wallenberg Centre for Molecular Medicine, Umeå University, 901 85 Umeå, Sweden; [f]New York University Winthrop Hospital, Mineola, NY 11501; and [g]Howard Hughes Medical Institute, Chevy Chase, MD 20815

Contributed by Richard O. Hynes, August 6, 2019 (sent for review May 28, 2019; reviewed by Wilhelm Haas and Lynn Matrisian)

Pancreatic ductal adenocarcinoma (PDAC) has prominent extracellular matrix (ECM) that compromises treatments yet cannot be nonselectively disrupted without adverse consequences. ECM of PDAC, despite the recognition of its importance, has not been comprehensively studied in patients. In this study, we used quantitative mass spectrometry (MS)-based proteomics to characterize ECM proteins in normal pancreas and pancreatic intraepithelial neoplasia (PanIN)- and PDAC-bearing pancreas from both human patients and mouse genetic models, as well as chronic pancreatitis patient samples. We describe detailed changes in both abundance and complexity of matrisome proteins in the course of PDAC progression. We reveal an early up-regulated group of matrisome proteins in PanIN, which are further up-regulated in PDAC, and we uncover notable similarities in matrix changes between pancreatitis and PDAC. We further assigned cellular origins to matrisome proteins by performing MS on multiple lines of human-to-mouse xenograft tumors. We found that, although stromal cells produce over 90% of the ECM mass, elevated levels of ECM proteins derived from the tumor cells, but not those produced exclusively by stromal cells, tend to correlate with poor patient survival. Furthermore, distinct pathways were implicated in regulating expression of matrisome proteins in cancer cells and stromal cells. We suggest that, rather than global suppression of ECM production, more precise ECM manipulations, such as targeting tumor-promoting ECM proteins and their regulators in cancer cells, could be more effective therapeutically.

PanIN | pancreatitis | PDAC | ECM

Patient survival in pancreatic ductal adenocarcinoma (PDAC) remains among the lowest of all common cancers, with 5-y survival rate less than 8% (1). Various therapeutic efforts have yielded only limited improvements in patient survival over the past few decades. A hallmark of pancreatic cancer is highly fibrotic stroma, which constitutes a major fraction of the tumor mass. PDAC fibrosis compromises drug delivery, hampers immune cell access, and promotes resistance to cytotoxic therapies (2–5). Nonselective depletion of tumor-associated stroma using inhibitors of the Hedgehog pathway (4) or targeted depletion of hyaluronan (HA) by PEGylated-hyaluronidase (6), both enhanced drug uptake and stabilized the disease in preclinical mouse models, at least transiently. However, clinical trials of Hedgehog pathway inhibitors in metastatic PDAC failed to provide any therapeutic efficacy, and phase 2 clinical trials with such inhibitors were halted because of paradoxical acceleration of disease progression (7). Preclinical studies in mouse PDAC had revealed successful depletion of stromal elements upon long-term inhibition or genetic ablation of Hedgehog signaling, as well as depletion of α-smooth muscle actin-positive stromal cells. However, tumor cells were less differentiated (8, 9), and the mice demonstrated signs of severe cachexia (8), resulting in higher mortality. These data imply that the stromal microenvironment likely contains components that can either promote or restrain tumor progression. On the other hand, a phase 2 clinical trial of PEGPH20 showed improvement in progression-free survival of HA-high patients (10). Together, these clinical findings suggest that a more detailed understanding of stromal components could provide potential biomarkers for patient stratification, and targets for more focused interventions.

Extracellular matrix (ECM), as a major component of PDAC stroma, provides both biophysical and biochemical cues that regulate malignant cell behavior. Abnormal ECM in the tumor microenvironment not only triggers cancer progression by directly promoting cellular transformation and metastasis, but also affects stromal-cell behaviors, such as angiogenesis and inflammation, and can enhance formation of a tumorigenic microenvironment (11, 12). ECM proteins have also been recognized as important components of the metastatic niche to maintain cancer stem cell properties and enable outgrowth of metastasis-initiating cells (13–15). Sorting out the composition and changes of the ECM during PDAC progression, as well as the contributions of stromal and epithelial compartments to PDAC matrix, would guide the development and application of more precise PDAC therapies.

Significance

We describe here the most comprehensive analyses of extracellular matrix (ECM) of pancreatic ductal adenocarcinoma (PDAC) yet available, which detected previously unknown molecular changes during PDAC progression in both mouse models and human patients. These data distinguish ECM proteins produced by tumor cells from those produced by stromal cells and show that it is the diverse set of tumor cell-derived proteins that correlate best with poor patient survival. In contrast, the stroma-derived ECM proteins, which comprise the bulk of the microenvironmental ECM, include both proteins correlating with good survival and proteins correlating with poor survival. These data may help explain why prior nonselective depletion of the stroma led to poorer patient outcomes and suggest more precise ECM manipulations as PDAC treatments.

Author contributions: C.T., S.A.C., D.A.T., and R.O.H. designed research; C.T., K.R.C., D.Ö., S.R., Y.H., and M.G. performed research; C.T., K.R.C., and D.R.M. analyzed data; and C.T. and R.O.H. wrote the paper.

Reviewers: W.H., Harvard University Medical School; and L.M., Pancreatic Cancer Action Network.

The authors declare no conflict of interest.

Data deposition: The raw mass spectrometry data reported in this paper have been deposited in the public proteomics repository MassIVE, https://massive.ucsd.edu/ProteoSAFe/static/massive.jsp (accession ID MSV000082639).

[1]K.R.C. and D.Ö. contributed equally to this work.

[2]To whom correspondence may be addressed. Email: rohynes@mit.edu.

This article contains supporting information online at www.pnas.org/lookup/suppl/doi:10.1073/pnas.1908626116/-/DCSupplemental.

First published September 4, 2019.

The matrisome is defined as the combination of core ECM proteins, including collagens, glycoproteins, and proteoglycans, and ECM-associated proteins, such as ECM regulators (e.g., proteases and their inhibitors, cross-linking agents), ECM-affiliated proteins (e.g., mucins lectins, annexins), and secreted factors (e.g., growth factors, chemokines) (16). We have used liquid chromatography–tandem mass spectrometry (LC-MS/MS) to define the matrisome compositions of several normal and tumor tissues from mouse models of cancer, as well as human tumors (16–21), and such studies have revealed previously unknown, functionally relevant cancer promoters (17, 21).

To date, there have not been comprehensive analyses of the matrisome in progressive stages in PDAC patients. In this study, we applied quantitative MS-based proteomic approaches to examine systematically the composition and dynamics of ECM proteins during PDAC progression in both mouse PDAC models and human patient samples. High levels of ECM proteins derived from tumor cells, rather than those exclusively produced by stromal cells, tend to associate with poor patient survival, while different stromal-cell–derived ECM proteins can either positively or negatively correlate with survival. These results demonstrate that the detailed proteomic analysis of PDAC tumor ECM can distinguish clinically relevant and tumorigenesis-promoting ECM proteins, which are potential candidates for future focused therapeutic interventions.

Results

A Quantitative Proteomic Approach to Profile ECM Changes during PDAC Progression. To define ECM compositions and changes in the course of PDAC progression, we enriched ECM proteins from tissue and tumor samples from 2 mouse genetic models that recapitulate the different stages of PDAC progression as well as samples from human patients (Fig. 1 *A* and *B*). Mouse samples included histologically verified triplicates of normal pancreas, early and late pancreatic intraepithelial neoplasia (PanIN)-stage pancreas harvested from the slowly progressing LSL-Kras$^{G12D/+}$; Pdx1-Cre (KC) mice, and PDACs harvested from the LSL-Kras$^{G12D/+}$; LSL-p53$^{R172H/+}$; Pdx-1-Cre (KPC) mouse model (*SI Appendix*, Fig. S1 *A* and *B*). The human samples included normal human pancreas, PanIN pancreas, PDAC, and chronic pancreatitis (CP), which is a progressive inflammatory disease of the pancreas where a high level of fibrosis occurs (22) (*SI Appendix*, Fig. S1 *A* and *B*). Normal human pancreas samples came from patients who had undergone surgery for adenoma of the duodenum. The incidence of PanIN increases to 60% in pancreatitis, which is considered to be a risk factor for PDAC (23). In order to capture and compare matrix compositions for pancreatitis and PanINs, we chose pancreatitis samples with minimal incidence of PanINs based on histology (*SI Appendix*, Fig. S1*B*). PDAC samples came from patients without neoadjuvant treatment, which is known to alter tumor ECM (24).

ECM proteins were enriched from pancreatic tissues using a modified subcellular fractionation protocol and verified by immunoblots with antibodies against protein markers representing different subcellular fractions (16) (Fig. 1 *A* and *B*). For both human and mouse, the compositions of the ECM-enriched fractions were then characterized by LC-MS/MS using isobaric mass tagging with tandem mass tag (TMT) 10-plex reagents for quantification (*SI Appendix*, Fig. S1*C*). Total abundance of peptides derived from matrisome proteins comprised more than 90% of total precursor ion signal intensity, indicating successful enrichment of ECM and ECM-associated proteins (Fig. 1*C*). In PDAC progression and in pancreatitis, collagens were the most prominent group of proteins, comprising more than 90% of the ECM protein signals at all stages (Fig. 1 *C* and *D*). Fibrillar collagens COL1A1, 1A2, and 3A1 are the major collagens that contribute over 90% of all collagen mass in samples across all stages in the pancreas and increase 2.6-fold (range, 2.2 to 3.0) during progression from normal pancreas to PDAC (*SI Appendix*, Fig. S2 *A* and *B* and *Supplemental Materials and Methods*). Abundances of proteins in the various ECM categories, relative to collagens I and III, increased as PDAC progressed (Fig. 1*D*), indicating an increase in the complexity of the ECM over the course of PDAC progression on top of the overall increase in ECM (Fig. 2 *E* and *F*; *SI Appendix*, Fig. S3 *A* and *B*). In order to illustrate this increase in matrisome complexity, we present the data normalized to the levels of collagens I and III in subsequent analyses (*SI Appendix*, *Supplemental Materials and Methods*).

Detection of ECM Signatures Characteristic of Distinct Stages. The timeline for PDAC progression from initiation to metastatic disease can be nearly 2 decades, suggesting a wide window of opportunity for early detection (25). We therefore compared human PanIN ECM to normal pancreas ECM, and identified a set of 147 proteins overrepresented in the PanIN matrix (Fig. 2 *A* and *D*). Among these, most (136) were also further overrepresented in PDAC (Fig. 2 *B* and *D*), indicating that they represent early PDAC progression signatures that might be functionally relevant in PDAC progression and/or useful as biomarkers (Fig. 2 *A*, *B*, and *D* and Dataset S1D; also compare Fig. 3*E* to *SI Appendix*, Fig. S3*A*).

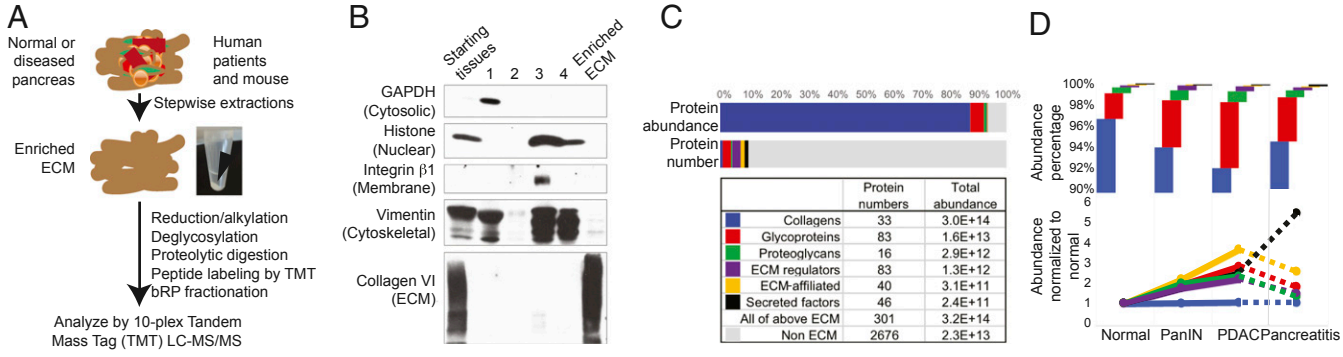

Fig. 1. Proteomic analysis of enriched ECM and ECM-associated proteins in human patient samples and genetically engineered mouse models. (*A*) Simplified schematic of the ECM enrichment and liquid chromatography–tandem mass spectrometry (LC-MS/MS)-based quantification of normal and diseased pancreas samples. See *Materials and Methods* for details. The arrow points to ECM pellet. (*B*) Western blot showing stepwise removal of cytosolic (1), nuclear (2), membrane (3), and cytoskeletal (4) fractions of proteins and final enrichment of ECM. Example shown is an extraction from a mouse KPC PDAC tumor. (*C*) Total abundance from summed precursor ion peak areas for all peptides (ion counts) and protein numbers from different groups of ECM and non-ECM proteins. Data from the human PDAC TMT set A (hA) are shown. (*D*) ECM from all stages has abundant collagens (>90%). An increase in the abundance of different groups of proteins relative to collagens I and III was observed in PanIN, PDAC, and CP ECM compared to normal pancreas. Abundance for each sample was calculated by splitting the combined precursor ion peak areas (MS1-based) in proportion to the individual reporter ion intensities (MS/MS-based) for each sample. Data from hA set are shown.

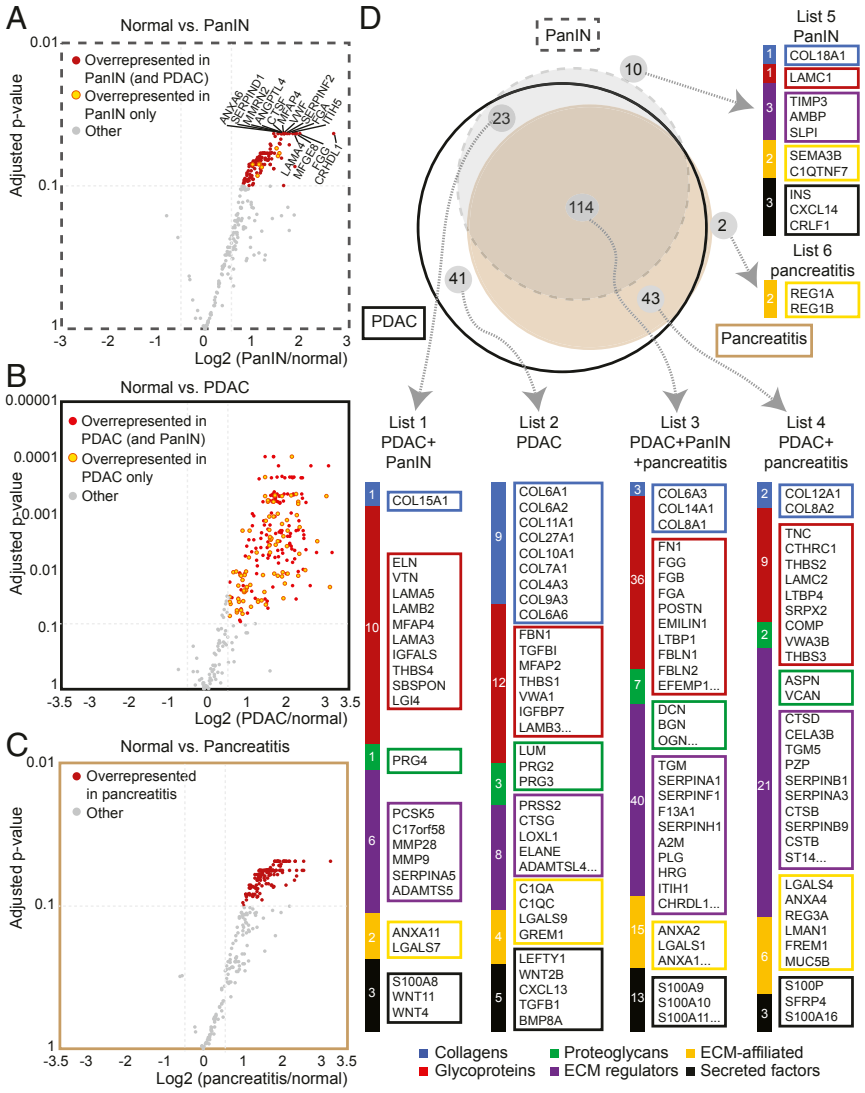

Fig. 2. Comparisons among diseased pancreas matrices and normal pancreas matrix. (*A*–*C*) Volcano plots comparing normal pancreas to PanIN (*A*), PDAC (*B*), and pancreatitis (*C*) of human samples using ECM protein TMT reporter-ion ratios to show the increase of many ECM proteins. Proteins with Benjamini–Hochberg 2-tailed *t* test adjusted *P* values less than 0.1 (*Materials and Methods*) and fold changes more than 1.5 are highlighted. Note that many proteins up-regulated in PanIN are further up-regulated in PDAC. (*D*) Venn diagram showing the overlap of significantly overrepresented proteins ($P_{adj} < 0.1$, fold change > 1.5) in each stage (Dataset S1D). The identities of the proteins in each field are shown; proteins in each matrisome category are ordered from the most abundant (*Top*) to the least abundant (*Bottom*), as decided by the mean abundance of the hA and hB sets. When there are too many proteins to list here, see Dataset S1D for complete information.

Pancreatitis and PDAC are both characterized by excessive stroma and are clinically difficult to distinguish (26, 27). We found that matrisome proteins significantly overrepresented in pancreatitis compared with normal are nearly exclusively (157/159) included among those overrepresented in PDAC and comprise around 3/4 of those (157/221), suggesting that matrix changes in pancreatitis represent a subset of the changes in PDAC (Fig. 2 *B*–*D* and Dataset S1D; also compare Fig. 3*E* to *SI Appendix*, Fig. S3*B*). PDAC, compared with PanIN and pancreatitis, up-regulates the largest set of matrisome proteins (Fig. 2*D*) and shows the biggest increase in matrisome protein abundance (Fig. 1*D*) and complexity (Fig. 2*D*); thus, PDAC represents the most fibrotic state.

We then compared the matrisome proteins, broken down into their categories, that are shared or specific to certain stage(s). Two out of 3 significantly overrepresented secreted factors shared by PanIN and PDAC, but not by pancreatitis, are WNT molecules (WNT11 and WNT4; Fig. 2*D*, list 1). Another WNT, WNT2B, is overrepresented in PDAC but not in PanIN or pancreatitis (Fig. 2*D*, list 2). Together, these data imply that WNTs may be specifically active in progression to PanIN and to PDAC, while this program may not be relevant in pancreatitis. There is a large group of relatively minor collagens that are overrepresented only in PDAC (9 collagens out of 41 total proteins in Fig. 2*D*, list 2, as compared to 16 collagens out of 233 total proteins in Fig. 2*D*; all lists combined). This result suggests that assembly of a diverse set of collagens is likely a late step of disease progression. Furthermore, the 2 pancreatitis-specific up-regulated proteins are REG1A and REG1B. They are known to be associated with islet development, beta-cell damage, diabetes, and pancreatitis (28). Thus, while the 3 disease states (PanIN, PDAC, and pancreatitis) share many or most matrisome proteins, there are characteristic matrisomal differences that distinguish them.

Human Patient and Mouse PDAC Share Similar ECM Compositions and Changes. Mouse genetic models have been used in preclinical testing of PDAC drugs, and the KPC model is one of the most widely used (29). We therefore sought to compare the composition of mouse and human PDAC ECM. Hierarchical clustering of the

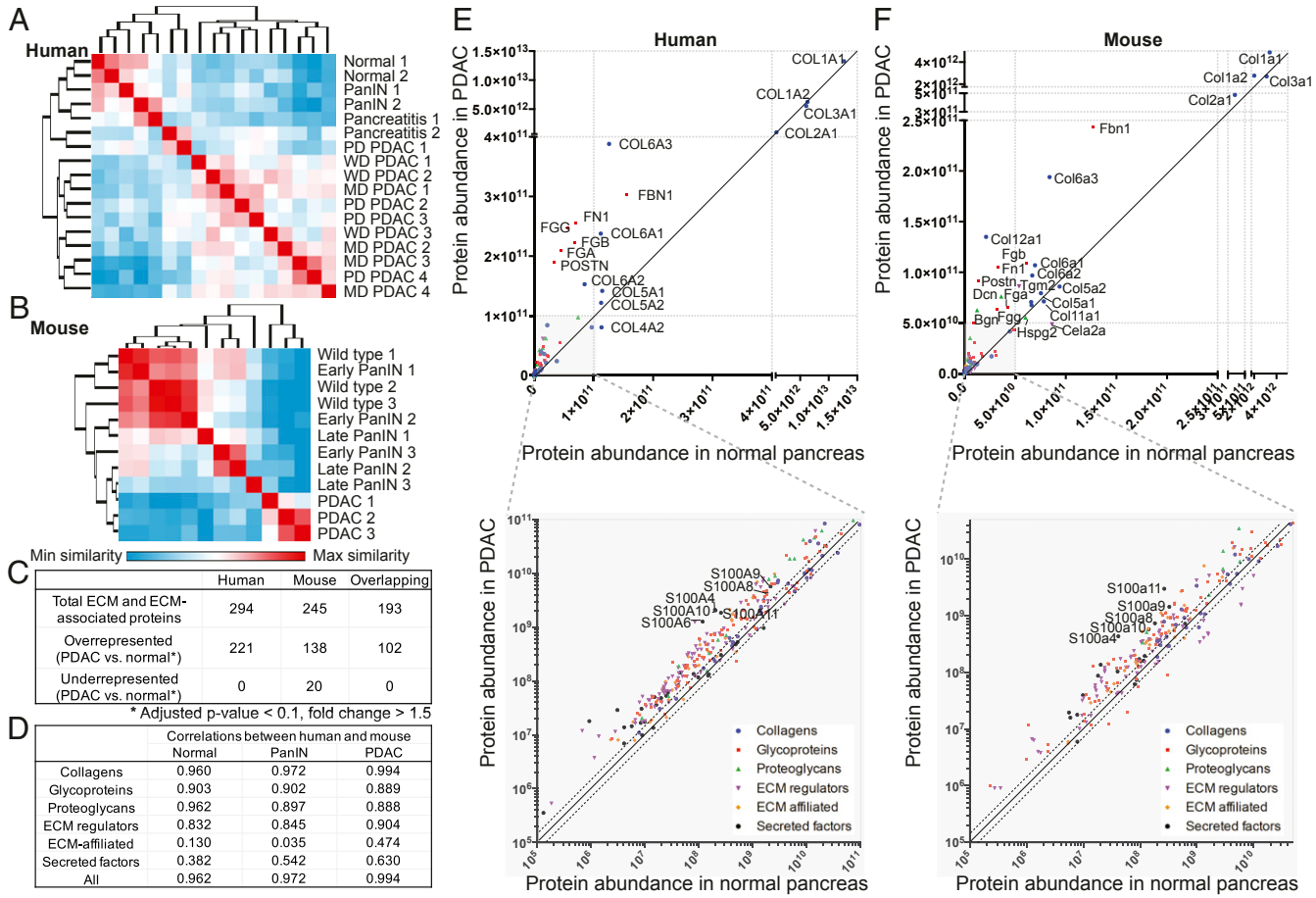

C

	Human	Mouse	Overlapping
Total ECM and ECM-associated proteins	294	245	193
Overrepresented (PDAC vs. normal*)	221	138	102
Underrepresented (PDAC vs. normal*)	0	20	0

* Adjusted p-value < 0.1, fold change > 1.5

D

	Correlations between human and mouse		
	Normal	PanIN	PDAC
Collagens	0.960	0.972	0.994
Glycoproteins	0.903	0.902	0.889
Proteoglycans	0.962	0.897	0.888
ECM regulators	0.832	0.845	0.904
ECM-affiliated	0.130	0.035	0.474
Secreted factors	0.382	0.542	0.630
All	0.962	0.972	0.994

Fig. 3. Comparisons of global changes in ECM and ECM-associated proteins in the course of PDAC progression in human and mouse. Hierarchical clustering of the protein-level TMT ratios by Pearson correlation using all identified matrisome proteins grouped almost all PDAC samples separately from normal and PanIN samples in both human (*A*) and mouse (*B*). Over 200 ECM and ECM-associated proteins were identified from both human and mouse sets (*C*), with a majority being significantly overrepresented ($P_{adj} < 0.1$) in PDAC compared to normal. Only proteins identified in both pairs of TMT MS (hA and hB for human; mA and mB for mouse) were included. Note that collagens I and III are the most prevalent proteins overall. (*D*) Pearson correlation analysis showed that core matrisome proteins (collagens, glycoproteins, and proteoglycans) and ECM regulators have the best correlations between mouse and human in normal, PanIN, and PDAC stages. Input was the abundance of all individual proteins identified in both sets of TMT MS for human and mouse. (*E* and *F*) Comparisons of protein abundance in normal pancreas and PDAC from human (*E*) and mouse (*F*). Proteins above the diagonal line are selectively overrepresented in PDAC. The gray regions are enlarged and plotted on a log scale to show all proteins. The dotted lines parallel to the diagonal line on the log-scale plots indicate 1.5-fold more (*Top* line) or less (*Bottom* line) than normal samples. Note the good agreement between human and mouse data with respect to up-regulated proteins.

protein-level TMT ratios grouped PDACs in a separate clade from normal pancreas, PanINs, or pancreatitis in both human (10/11 PDAC) and mouse (3/3 PDAC) samples (Fig. 3 *A* and *B*). These and prior figures indicate that PDAC tumors have qualitatively and quantitatively different ECM from normal pancreas, PanINs, and pancreatitis. In total, we identified comparable numbers of matrisome proteins from both human and mouse (294 vs. 245, respectively; Fig. 3*C* and Dataset S1). Among these, a major fraction (193) overlapped between human and mouse. There is also marked overlap between significantly overrepresented matrisome proteins in PDAC in human and mouse (Fig. 3*C*). Pearson correlation analyses showed that human patient and mouse model ECM compositions were highly correlated throughout PDAC progression, especially in the categories that comprise or regulate core matrisome proteins, including collagens, glycoproteins, proteoglycans, and ECM regulators (Fig. 3*D*).

Plotting the top 5 most abundant proteins from each matrisome category of both species against stages of PDAC progression showed that the most abundant proteins comprising the tissue matrices were similar, in both abundances and alterations, between human and mouse in the categories of collagens, glycoproteins, and proteoglycans, but that ECM regulators, ECM-affiliated proteins, and secreted factors showed somewhat more variation (*SI Appendix*, Fig. S2 *A* and *B*).

Focusing specifically on comparisons between normal pancreas and PDAC, many matrisome proteins are significantly overrepresented in PDAC compared to normal in both human (lists 1 to 4 in Fig. 2*D*) and in mouse, and many of these are common between the 2 species (Fig. 3 *E* and *F*). For example, the following features are shared between human and mouse: fibrillar collagens COL1A1, COL1A2, and COL3A1 are the most abundant collagens at all stages, while COL6A3 (and to a lesser extent COL6A1/A2) is highly overrepresented in PDAC; Fibrillin-1 (FBN-1), fibronectin (FN1), fibrinogens (FGA, FGB, and FGG), and periostin (POSTN) are the most abundant glycoproteins, and they are all overrepresented in PDAC; S100 family members are the most abundant and overrepresented secreted factors in PDAC. Immunohistochemistry confirmed many of the significantly overrepresented proteins in PDAC compared to normal pancreas in both human and mouse (*SI Appendix*, Fig. S4). Overall, these data not only disclosed the major compositions of normal and diseased pancreas ECM but also revealed a high degree of resemblance between human patients and

the KC/KPC mouse models in the ECM changes during PDAC progression.

Stromal Cells Make Most of the Bulk ECM. It is crucial to understand the cellular origin of the matrisome proteins to delineate their functions. Therefore, we generated human-to-mouse orthotopic xenograft tumors in NOD/SCID/IL2Rγ-null (NSG) mice using AsPC1 and BxPC3 human PDAC cell lines, as well as HuO1 and HuO2 human organoid lines (30), and applied unlabeled LC-MS/MS analyses on the enriched ECM proteins (Fig. 4*A*). From the MS results, we assigned cellular origins based on the peptide sequence differences between human and mouse: human-derived proteins are made by cancer cells, while mouse-derived ones are made by stromal cells. A limitation of this system is that we do not capture matrisome proteins contributed or induced by many immune cells because these experiments required immunocompromised NSG mice.

We assigned cellular origins to 220 matrisome proteins, seen in at least 2 out of the 4 classes of xenotransplant tumors and identified by at least 2 species-distinguishing peptides (Fig. 4*A*). We defined individual proteins to be cancer-cell or stromal-cell derived when at least 90% of the ECM peptide abundance was derived from human or mouse, respectively, and defined all of the others as "both-derived." We assigned tumor vs. stromal-cell origins to 180 of 294 human patient matrisome proteins (Fig. 4*A* and *SI Appendix*, Fig. S5*D*, columns 1, 2, 3, and 4). Among these, a higher proportion of glycoproteins, proteoglycans, and ECM regulators are stroma-derived; collagens, ECM-affiliated proteins, and secreted factors come from both cancer cells and stromal cells (*SI Appendix*, Fig. S5*D*, columns 5, 6, and 7).

Stromal cells make most of the ECM mass across all 4 types of xenograft tumors, and stroma from organoid-derived xenograft tumors makes more ECM than that from 2D cell-line–derived tumors (Fig. 4*B*). Pearson correlation showed that organoid-xenograft ECMs resemble human PDAC ECM slightly more closely than do 2D cell-line-xenograft ECMs, although all are similar (*SI Appendix*, Fig. S5*A*). We further found that stromal cells generate predominantly core matrisome components (collagens, glycoproteins, and proteoglycans), while the tumor cells make a wider diversity of all categories of matrisome proteins (Fig. 4 *C* and *D*). Cancer-cell–derived matrices are not closely similar among 2D lines and organoids (*SI Appendix*, Fig. S5*B*), but they appear to induce very similar stromal-cell–derived ECM components (*SI Appendix*, Fig. S5*C*).

Cancer-Cell–Derived Matrisome Proteins Correlate with Short Patient Survival. ECM proteins can affect tumor progression and patient survival, by promoting tumor cell proliferation, survival, and metastatic spread (17, 31). However, the functions of ECM proteins have not been assessed in the context of their origins. Here, we wanted to examine systematically the correlations between patient survival and ECM proteins of different cellular origins. To examine patient survival, we calculated Cox regression *P* values and hazard ratios for each of the most significantly overrepresented ECM proteins identified from our human patient TMT MS datasets (Dataset S3). We compared overall survival of patients within the top quartile (25%, $n = 44$) with those within the bottom quartile (25%, $n = 44$) of gene expression in The Cancer Genome Atlas (TCGA) pancreatic cancer dataset (179 patients; http://www.cbioportal.org/). A sizeable number of cancer-cell–derived and both-derived ECM proteins that are overexpressed in human PDAC, correlated with short patient survival, and none correlated with good survival. In contrast, among stromal-cell–derived matrisome proteins, some correlated positively, and others negatively, with patient survival (Fig. 5 *A* and *C*, *SI Appendix*, Fig. S6, and Dataset S3). We then examined survival in an independent dataset of 65 PDAC patients, samples from which have at least 40% epithelial cellularity (32). We arrived at a similar conclusion that ECM proteins made by cancer cells tend to correlate with poor patient survival, whereas among ECM proteins exclusively derived from stromal cells, some correlate with good survival and some with poor survival (Fig. 5 *B* and *C*, *SI Appendix*, Fig. S6, and Dataset S3). Matrisome proteins in the categories of ECM regulators, ECM-affiliated proteins, and secreted factors are cancer-cell- and both-derived and correlated with poor patient survival. Stromal-cell-made proteoglycans, on the other hand, correlate with good patient survival (Fig. 5*C* and Dataset S3). Together, these results lead to the interesting conclusion that, although the bulk of matrisome proteins are derived from stromal cells, cancer cells secrete matrisome proteins that appear to be protumorigenic while individual stromal-cell–derived matrisome proteins appear either to support or restrain tumor progression.

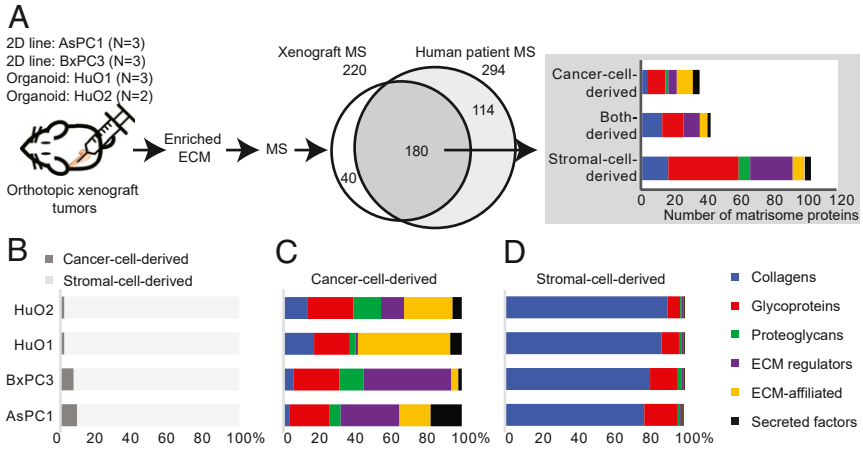

Fig. 4. Definition of matrisome proteins derived from cancer cells and stromal cells and their characterization. (*A*) Schematic overview of the xenograft ECM MS experiment. Venn diagram shows cell-of-origin assignments for a large fraction (180/294) of ECM proteins identified from human patients. "Human patient MS" group includes proteins that are identified in both *A* and *B* sets of TMT MS analyses (*SI Appendix*, Fig. S1*C*). "Xenograft MS" group includes proteins that are detected in at least 2 out of 4 xenograft lines, and by at least 2 species-specific peptides. On the *Right*, the numbers of matrisome proteins are broken down into their cellular origins, and their matrisome categories are also shown. (*B*) Stromal cells (mouse) contribute more ECM mass than do cancer cells (human), even more so in organoid lines (HuO1, HuO2) as compared with 2D lines (AsPC1, BxPC3). Abundances calculated from summed precursor ion chromatographic peak area of LC-MS/MS peptides. (*C* and *D*) Cancer-cell–derived ECM includes proteins from all ECM categories (*C*), while stromal cells primarily make collagens and glycoproteins (*D*).

Probing the ECM Reveals Differential Activation of Major Signaling Pathways in Cancer-Cell and Stromal-Cell Compartments. We next sought to investigate whether the expression of the ECM proteins in different cell types was controlled by differential upstream regulators and pathways. We used Ingenuity Pathway Analysis (IPA) to identify presumptive regulators in cancer cells and stromal cells, by analyzing 2 lists, comprising proteins that are significantly overrepresented in human PDAC and can be synthesized by 1) cancer cells or 2) stromal cells, respectively (Dataset S4). From these analyses, we identified regulators and pathways that are potentially active in regulating matrisome protein expression by the cancer-cell and stromal-cell compartments.

TGFB1 appears to be the factor potentially regulating the greatest number of matrisome proteins in both cancer cells and stromal cells (Fig. 5*D* and Dataset S4, Tab 2). TGF-β signaling is known to regulate expression of many matrisome proteins and

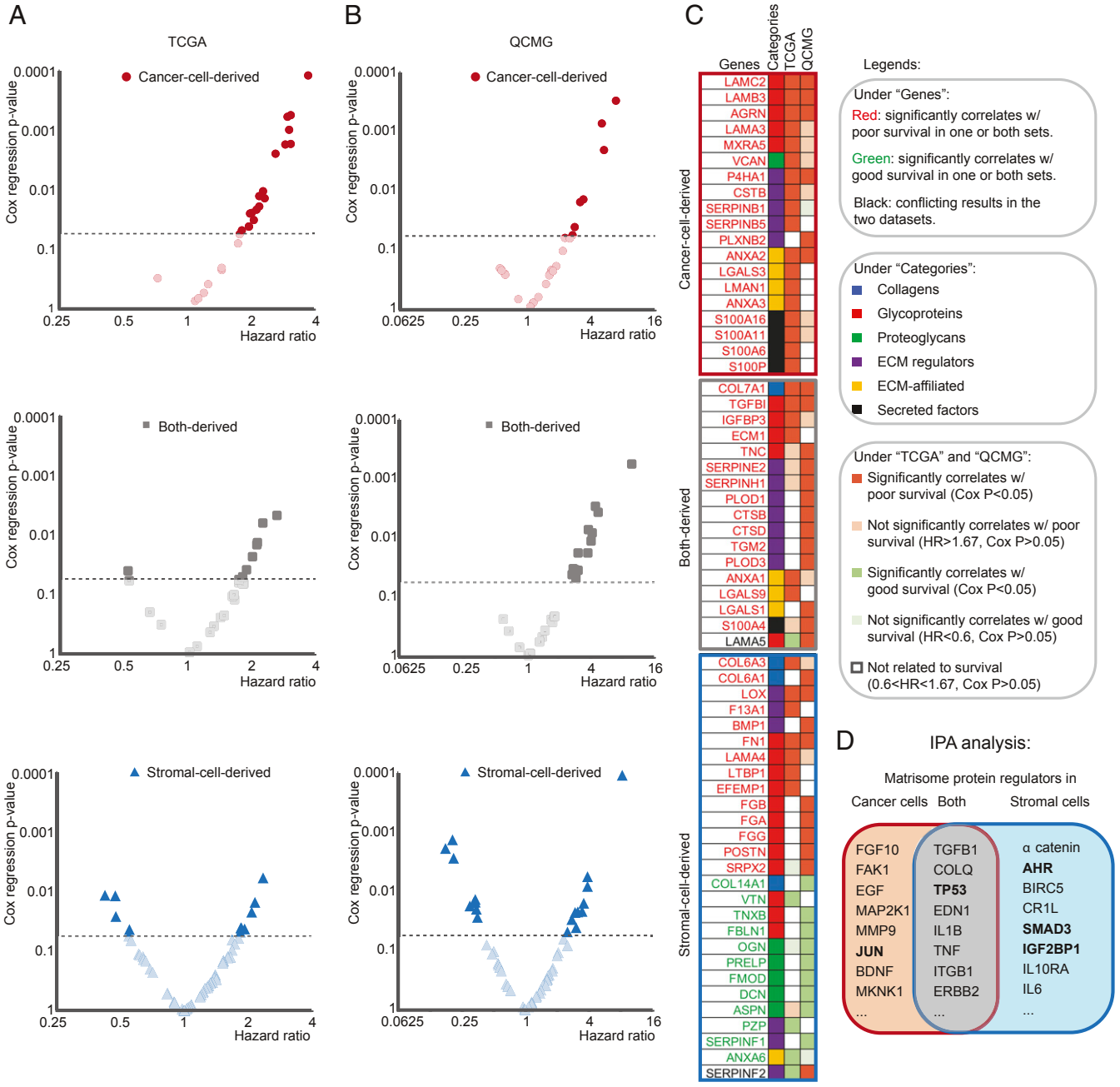

Fig. 5. Survival and pathway analyses on matrisome proteins derived from cancer cells and stromal cells. (*A* and *B*) ECM proteins significantly overrepresented in human PDAC TMT MS comparing PDAC to normal with $P_{adj} < 0.02$ were tested against both TCGA (*A*) and QCMG (*B*) human PDAC datasets. Cancer-cell–derived proteins (red) and both-derived proteins (gray) correlated with small Cox regression *P* values and large hazard ratios (HRs), indicative of short survival. In contrast, many stroma-derived proteins (blue) tend to correlate with good survival (low hazard ratio). Proteins that do not significantly correlate with survival (Cox regression $P > 0.05$) are grayed out in *Lower* part of figure. (*C*) The identity of the proteins that significantly correlate with survival (Cox regression $P < 0.05$). Refer to color legends in the figure for the meaning of the color coding of each column. (*D*) Ingenuity Pathway Analysis (IPA) was performed on proteins that are overrepresented in PDAC and made by cancer cells and/or stromal cells (*Materials and Methods*). The top 8 predicted regulators of the significantly overrepresented matrisome proteins exclusively in cancer cell and stromal cells, as well as in both compartments, are shown. Refer to Dataset S4 for the complete lists of regulators. The bolded genes are predicted direct regulators.

play important pleiotropic roles in cancer progression (33, 34). Among the regulators that are active in cancer cells but not stromal cells in our analysis (*Materials and Methods*), FGF10, FAK1, and EGF are the top 3 most strongly predicted regulators of matrisome proteins (Fig. 5*D*). The 6 matrisome proteins that are predicted to be regulated by FGF10 all correlate with poor patient survival, which suggests that FGF10 may be an important protumorigenesis factor that is active in cancer cells (Dataset S4, Tab 3, and *Discussion*). In the stromal cells, IL6 and IL10RA signaling pathways score as high-ranking potential regulators for matrisome protein expression, along with a few other regulators that have not been studied previously in PDAC, such as AHR and CR1L. Altogether, IPA analysis suggests that different signaling pathways may function within the tumor cells or stromal cells to regulate matrisome protein expression in PDAC. The pathways that are active in cancer cells represent potential targets for therapeutic intervention, whereas caution should be exercised when targeting pathways that are also active in stromal cells.

Discussion

The role of the ECM in cancer is of long-standing and increasing interest. In this study, we used proteomics to define multiple changes in ECM profiles in the course of PDAC progression in both the KC/KPC mouse models and in human patient samples. We observed marked increases in both abundance and complexity of ECM as PDAC progresses, concordant with the increasing level of desmoplasia. We describe early changes in matrix proteins, commencing at the PanIN stage, which could potentially be used for early detection biomarkers. Furthermore, using MS analysis of xenografts, we systematically assigned cancer-cell vs. stromal-cell origins to a majority of the ECM and ECM-associated proteins discovered in human PDAC. This analysis revealed that, although the bulk of the ECM mass is derived from stromal cells, significantly more ECM proteins produced by the tumor cells correlate with poor prognosis.

Complex Changes in ECM Composition. PDAC is one of the most desmoplastic cancers. ECM in PDAC has been acknowledged to be functionally important yet not comprehensively understood. Some previous proteomic studies identified differentially expressed proteins in PDAC patient samples and normal pancreas (35–37). However, these studies used the entire tissues and only identified limited numbers (≤10) of matrisome protein changes, which suggests that ECM enrichment, as used here, is necessary for a more complete assessment of ECM changes. A recent compartment-resolved proteomic study on a different KTC mouse PDAC model that carries $Kras^{G12D}$ and has loss of Tgfbr2 (38) observed fibrosis and inflammation markers being up-regulated in PDAC. In our study, we carefully selected samples from the different progression stages and tumor differentiation levels in both human and mouse. We also modified the ECM enrichment protocol to suit pancreatic tissue characteristics (high zymogens for normal pancreas, and high level of fibrosis for PDAC) to successfully deplete abundant cytoskeleton proteins and histones, which are the usual contaminants for enriched ECMs, while retaining matrisome proteins. In fact, over 90% of the protein abundance in our analyses came from matrisome proteins (Fig. 1*C*). We identified a large number of matrisome proteins: 294 for human and 245 for mouse (Fig. 3*C*), which is higher than reported in the analysis of KTC mouse PDAC tumors (38) or than has usually been identified from other types of tumors (17, 18, 21). The latter difference could also be partly due to the high complexity and desmoplastic characteristic of PDAC.

The KC/KPC mouse models have been used as primary preclinical models for PDAC drug development. The data presented here show that human PDAC and KC/KPC mouse models are very similar in their ECM profiles and in their changes during PDAC progression. They share not only the most abundant proteins in each of the core matrisome categories, but they also up-regulate similar proteins during PDAC progression, such as COL6, FN1, and TNC (Fig. 2*D*, lists 2 to 4). There are, however, some differences between human and mouse matrices. For example, mice express more Col12a1 than humans in PDAC (Fig. 3 *E* and *F*), and TIMP3 is abundant in normal and diseased pancreas in human but not mouse (*SI Appendix*, Fig. S2 *A* and *B*). The ECM-affiliated proteins and secreted factor profiles are also significantly different between human and mouse (*SI Appendix*, Fig. S2 *A* and *B*). Our study comprehensively compares the matrisome proteins in the KC/KPC mouse models and human patients, and one should be aware that differences in the ECM may lead to differential efficacies between preclinical and clinical drug tests.

Comparisons among PanIN, PDAC, and Pancreatitis. We aimed to resolve the PDAC ECM changes along a temporal axis. PanIN-stage pancreas up-regulates a panel of matrisome proteins, and they likely represent an early response to transformed neoplastic cells. Serum proteins, fibrinogens (FGA and FGG), and VWF are overrepresented in PanIN ECM, perhaps suggestive of an early activation of a "wound-healing program" in the pancreas. The deposition of provisional fibrin-rich matrix could promote neoplastic cell migration and induce angiogenesis (39). Many of the significantly up-regulated matrisome proteins in PanIN ECM have not previously been implicated in PDAC. For example, we observed up-regulation of CHRDL1, a known antagonist of BMP4 signaling and a tumor suppressor in breast cancer (Fig. 2*A* and *SI Appendix*, Fig. S3*A*) (40). It is unclear what role CHRDL1 may play in the progressing stage of PDAC.

ECMs from pancreata exhibiting PanIN and pancreatitis, although less abundant than ECM in PDAC (Fig. 1*D*), both showed increases in similar and highly overlapping sets of proteins with those in PDAC matrix (Fig. 2*D*). Moreover, cell lines of different genotypes, such as the BxPC3 line (wild-type Kras gene) and AsPC1 line (mutated Kras gene) (41), as well as human PDAC organoids, induce very similar ECM protein expression in the xenograft tumors (*SI Appendix*, Fig. S5*A*). Here, we have the advantage of distinguishing cancer-cell– vs. stromal-cell–derived matrix. We observe that, although the ECM proteins made by the cancer cells can differ in vivo (*SI Appendix*, Fig. S5*B*), the stromal cells upon induction express highly similar matrisome protein profiles (*SI Appendix*, Fig. S5*C*). This implies that various perturbations in the pancreas, including oncogenic transformation and chronic inflammation, can lead to similar stromal reactions to build up a dense stroma, which one could think of as a wound or inflammatory response.

Stromal-Cell–Derived ECM Proteins Appear Correlated with Either Good or Poor Prognosis. The dense stroma in PDAC has been suggested to hamper drug delivery and to be immunosuppressive. How to treat this high fibrosis state has been a focus of study. We know now that nonselective ablation of the stromal ECM response, for example by inhibition of hedgehog-pathway signaling, leads to more aggressive cancer cells, implying that the dense stroma in PDAC may be a double-edged sword (8, 9). The mechanisms underlying the acceleration of cancer progression are not fully understood. In this study, we discovered that, unlike cancer cells, stromal cells express matrisome proteins that correlate with both good and poor prognosis in patients. This suggests that stromal cells build matrix in the tumor microenvironment that can both promote and restrain cancer progression. Many of the highly expressed, stromal-cell–derived proteins that correlate with poor survival in the Queensland Centre for Medical Genomics (QCMG) dataset are small leucine-rich proteoglycans (SLRPs), including osteoglycin (OGN), PRELP, fibromodulin (FMOD), decorin (DCN), and asporin (ASPN) (Fig. 5*C* and Dataset S2).

DCN has been shown to inhibit tumor cell growth by physically antagonizing receptor tyrosine kinase signaling; furthermore, DCN and FMOD are TGF-β binders and blockers (42, 43). Although not in our list of survival-correlated proteins, lumican (LUM) is another SLRP produced by stromal cells (Dataset S2) that is significantly up-regulated in human PDAC ECM (Dataset S1D) in this study. Stromal expression of LUM has been shown to reduce metastasis and prolong PDAC patient survival through mechanisms including inhibition of EGFR signaling by promoting its internalization (44) and inducing a quiescent cell state (45).

PDAC can be subcategorized into different genotypic subgroups, and these could result in differential stromal contents (32, 46). Heterogeneity exists not only in cancer cells but also at the level of tumor-associated fibroblasts in various types of cancer (47–51). Fibroblasts exist as phenotypically and functionally distinct groups (47, 49, 51). It will be intriguing to investigate whether the different functional subtypes of fibroblasts secrete different combinations of matrisome proteins, especially ones correlated with good or poor survival, through methods such as single-cell mRNA sequencing in human PDAC tumors (52).

In conclusion, when designing therapeutic strategies, one should be cautious in assessing the net effect of the dense desmoplasia and, rather than global targeting of ECM, case-by-case assessment of individual ECM proteins as targets is needed. For example, single-agent hyaluronidase treatment in PDAC patients seemed to improve progression-free survival in a phase II clinical trial (10), although HA is a linear polysaccharide and thus was not assessed by our protein-focused MS analyses.

Tumor Cell-Derived ECM Proteins Appear Best Correlated with Poor Prognosis. Cancer cells, on the other hand, make less than 10% of the ECM mass. However, we found that a number of cancer-cell–derived matrisome proteins correlate with poor patient survival, whereas very few correlate with good prognosis. Consequently, cancer-cell–derived matrisome proteins could be attractive therapeutic candidates. However, it is important to note that correlation does not mean causation, and these candidate ECM proteins need to be assessed for their functional involvement in cancer progression.

IPA revealed different pathways and regulators that potentially drive matrisome gene expression in cancer cells and stromal cells. FGF, FAK1, and EGF score as the top 3 regulators potentially active in cancer cells but not in stromal cells. Consistent with our finding, previous studies showed that stroma-derived FGF10 could activate its receptor FGFR2 expressed on the PDAC cancer cells to induce migration and invasion, correlating with poor patient survival (53). FAK1 has also been shown to be active in neoplastic PDAC cells and to correlate with an immunosuppressive tumor microenvironment and poor patient survival. Consequently, inhibition of FAK has been proposed to be a promising therapeutic regimen for PDAC (54). Factors downstream of EGFR in pro-oncogenic signaling pathways, including JUN, MAP2K1, MKNK1, and ERK, are predicted to be regulators of matrisome proteins in cancer cells (Fig. 5*D* and Dataset S4). EGFR has been shown to be overexpressed or overactivated in multiple types of cancer cells, including PDAC cells, to promote tumorigenesis (55–57). Erlotinib, a targeted EGFR inhibitor, was tested in a phase III clinical trial in advanced PDAC and slightly improved overall survival as the primary endpoint, resulting in Food and Drug Administration approval for the combination of gemcitabine plus erlotinib (58). The result of this clinical trial is consistent with our finding that targeting regulators that regulate cancer-cell–derived matrisome proteins may be beneficial to PDAC patients.

Conclusions

Our proteomic analysis defined multiple levels of matrix changes during PDAC progression, including increasing ECM diversity, as well as the similarity of mouse PDAC models with the human disease. Importantly, we delineated the different contributions of matrix proteins made by cancer cells or stromal cells. Although the bulk of the desmoplastic ECM is produced by the stromal cells, tumor cells also themselves produce diverse ECM proteins, and these, in particular, correlate with short patient survival. Meanwhile, the bulk stroma-derived ECM components include proteins that correlate with either short or long survival.

Our study suggests the need for more precise targeted interventions. When choosing interventions to deplete the bulk of matrix, one ought to pay attention to good survival-correlated stromal proteins and/or cells that make them. On the other hand, cancer-cell–derived ECM proteins, or their regulators, could be potential candidates for therapeutics.

Materials and Methods

Mouse Strains and Samples. The Massachusetts Institute of Technology (MIT) and Cold Spring Harbor Laboratory (CSHL) Animal Care and Use Committees reviewed and approved all animal studies and procedures. KPC and KC mouse models were on C57BL/6J background. Samples representing early and late PanIN stages were collected from KC mice at 3 and 9 mo of age, respectively. Three nonadjacent pieces of pancreas were sectioned and examined histologically, and pancreata with at least 2/3 pieces having the expected lesions were selected. PDAC tumors were collected from tumor-bearing KPC mice. All samples were snap-frozen when collected.

Human Samples. All participating individuals provided written informed consent. The study was conducted in accord with the Helsinki Declaration of 1975 and was approved by the regional research ethics board of northern Sweden (Dnr. 09-175M/2009-1378-31). Human PDAC tissues were collected from patients undergoing Whipple's procedure. Normal pancreatic tissues were collected from patients with adenomas in the duodenum; CP samples were from patients with severe and symptomatic CP, and PanIN lesions were from patients with adenomas in the duodenum or benign lesions in the pancreas where adjacent pancreatic tissue showed no other pathology than PanIN. Tissue samples were snap-frozen in liquid nitrogen directly after collection and examined by 2 independent pathologists before inclusion in the study.

Orthotopic Implantation from 2D Cell Culture. For xenograft tumor experiments, 5×10^5 AsPC1 or BxPC3 cells in 50 μL of PBS were injected into pancreata of 8- to 10-wk-old NOD/SCID/IL2Rγ-null (NSG) mice (The Jackson Laboratory). Tumors were harvested 6 wk post injection.

Organoid Culture and Implantation. All human organoid experiments were approved by the institutional review boards of Memorial Sloan Kettering Cancer Center and CSHL, and all subjects taking part in the study provided written informed consent. Organoids were isolated as previously described; briefly, tumor tissue was digested with collagenase II (5 mg/mL; Gibco) for 12 h at 37 °C in "human complete medium" as published in Boj et al. (30). Tissue was further digested for 15 min at 37 °C in TrypLE (Gibco). The cells in suspension were seeded in Matrigel with human complete medium on top to establish organoids. After expansion, $\sim 0.5 \times 10^6$ cells were spun down, suspended in 50 μL of PBS, and injected orthotopically into pancreata of 6- to 8-wk-old NSG mice (30). Palpable tumors larger than 8 mm were harvested.

ECM Protein Enrichment from Pancreatic Tissues. The ECM enrichment method was modified from previous studies (16). In brief, we used the CNMCS compartment protein extraction kit (Millipore) to decellularize tissue samples ranging from 50 to 100 mg. Frozen samples were homogenized with a Bullet Blender (Next Advance). The stiff PDAC samples were first finely minced manually with scissors for better homogenization results. The lysates were then incubated in a series of buffers to remove sequentially: 1) cytosolic, 2) nuclear, 3) membrane, and 4) cytoskeletal proteins. One modification from the kit protocol and the protocol previously published (59) is that we used 20% CS plus 80% M buffer instead of 100% CS buffer for removal of cytoskeletal proteins for better retention of ECM proteins in pancreatic tissues. The remaining insoluble pellet is the ECM-enriched fraction. The effectiveness of the ECM protein enrichment was monitored by immunoblotting.

Protein Digestion, Peptide Fractionation, TMT Labeling, and Quantitative MS. ECM-enriched fractions were solubilized in 8 M urea, disulfide bonds reduced and alkylated, and proteins deglycosylated with PNGaseF and digested with

Lys-C, and trypsin at 37 °C, all as previously described (17). Detailed information about the compositions of the 4 TMT 10-plexes (human 10-plexes A and B and mouse 10-plexes A and B), and TMT labels used is given in *SI Appendix*, Fig. S1*C*). Details of quantitative MS, as well as protein abundance quantification and domain analysis, are provided in *SI Appendix, Supplemental Materials and Methods*.

Survival Analysis. Gene expression and clinical data for human PDAC (both TCGA and QCMG) were downloaded from cBioportal (32). Gene expression data were *Z*-score normalized. For each profiled gene, we calculated the Cox proportional hazard regression *P* values and hazard ratios by determining the overall survival differences in categorized patients using quartile expression values (top vs. bottom quartile) for TCGA dataset ($n = 179$), and using all PDAC patients with continuous expression values for QCMG dataset ($n = 65$). The Cox regression analyses were done using the R package OIsurv.

IPA. IPA (https://www.ingenuity.com/products/ipa) was used to identify potential upstream regulators. The input lists included proteins that were significantly overrepresented in human PDAC and were synthesized by 1) cancer cells or by 2) stromal cells; those defined by MS data as both-derived were included in both input lists. The *P* value cutoff of 1E-5 was first applied to the 2 output lists, and then the filtered hits from both lists were compared to each other to assign regulators active in the cancer cells, stromal cells, or both compartments.

ACKNOWLEDGMENTS. We thank Jess Hebert and Noor Jailkhani for critical review of the manuscript; the Hope Babette Tang Histology Facility and Charlie Whittaker and Duanduan Ma of the Barbara K. Ostrom Bioinformatics and Computing Facility at the Koch Institute Swanson Biotechnology Center for assistance with bioinformatic analyses; Roderick Bronson for pathological analysis and Anette Berglund for technical assistance. C.T. was a Sherry and Alan Leventhal Family Fellow of the Damon Runyon Cancer Research Foundation. This work was supported by the STARR Cancer Consortium (to R.O.H. and D.A.T.), the Howard Hughes Medical Institute, of which R.O.H. is an investigator, and the Lustgarten Foundation, where D.A.T. is a distinguished scholar and director of the Lustgarten Foundation-designated Laboratory of Pancreatic Cancer Research. Support was also provided by National Cancer Institute (NCI) Cancer Center Support Grants to MIT, Koch Institute (P30CA14051-45), and Cold Spring Harbor (P30CA45508-27), and shared resources of the St. Giles Foundation Microscopy Center, Animal and Tissue Imaging, and the Animal Facility, both at CSHL. This work was also supported in part by grants from the NCI Clinical Proteomic Tumor Analysis Consortium Grants NIH/NCI U24-CA210986 and NIH/NCI U01 CA214125 (to S.A.C.) and NIH/NCI U24CA210979 (to D.R.M.). D.A.T. is also supported by the Cold Spring Harbor Laboratory Association, the NIH (5P30CA45508-27, 1U10CA180944-04, and 1R01CA190092-04, 5P20CA192996-03, 1U01CA210240-01A1), the Department of Defense (W81XWH-13-PRCRP-IA), and the V Foundation. S.R. and C.T. were supported by postdoctoral fellowships from the MIT Ludwig Center for Molecular Oncology. D.Ö. was supported by the Swedish Research Council (537-2013-7277 and 2017-01531), the Kempe Foundations (JCK-1301), the Swedish Society of Medicine (SLS-786661, SLS-691681, SLS-326921, SLS-250831, SLS-175991, and SLS-591551), federal funds through the county council of Västerbotten (ALFVLL369081, VLL-643451, and VLL-832001), the Cancer Research Foundation in Northern Sweden (AMP15-793, AMP 17-877, and LP 18-2202), the Swedish Foundation for International Cooperation in Research and Higher Education (PT2015-6432), the Knut and Alice Wallenberg Foundation, The Sjöberg Foundation, and the Swedish Cancer Society (CAN 2017/332 and CAN 2017/827).

1. R. L. Siegel, K. D. Miller, A. Jemal, Cancer statistics, 2018. *CA Cancer J. Clin.* **68**, 7–30 (2018).
2. M. A. Swartz, A. W. Lund, Lymphatic and interstitial flow in the tumour microenvironment: Linking mechanobiology with immunity. *Nat. Rev. Cancer* **12**, 210–219 (2012).
3. N. Hartmann *et al*., Prevailing role of contact guidance in intrastromal T-cell trapping in human pancreatic cancer. *Clin. Cancer. Res.* **20**, 3422–3433 (2014).
4. K. P. Olive *et al*., Inhibition of Hedgehog signaling enhances delivery of chemotherapy in a mouse model of pancreatic cancer. *Science* **324**, 1457–1461 (2009).
5. M. Yu, I. F. Tannock, Targeting tumor architecture to favor drug penetration: A new weapon to combat chemoresistance in pancreatic cancer? *Cancer Cell* **21**, 327–329 (2012).
6. M. A. Jacobetz *et al*., Hyaluronan impairs vascular function and drug delivery in a mouse model of pancreatic cancer. *Gut* **62**, 112–120 (2013).
7. D. Amakye, Z. Jagani, M. Dorsch, Unraveling the therapeutic potential of the Hedgehog pathway in cancer. *Nat. Med.* **19**, 1410–1422 (2013).
8. A. D. Rhim *et al*., Stromal elements act to restrain, rather than support, pancreatic ductal adenocarcinoma. *Cancer Cell* **25**, 735–747 (2014).
9. B. C. Özdemir *et al*., Depletion of carcinoma-associated fibroblasts and fibrosis induces immunosuppression and accelerates pancreas cancer with reduced survival. *Cancer Cell* **25**, 719–734 (2014).
10. B. A. Hingorani, Sr *et al*., Randomized phase II study of PEGPH20 plus nab-paclitaxel/gemcitabine (PAG) vs AG in patients (Pts) with untreated, metastatic pancreatic ductal adenocarcinoma. *J. Clin. Oncol.* **35**, 4008 (2017).
11. E. Cukierman, D. E. Bassi, Physico-mechanical aspects of extracellular matrix influences on tumorigenic behaviors. *Semin. Cancer Biol.* **20**, 139–145 (2010).
12. M. W. Pickup, J. K. Mouw, V. M. Weaver, The extracellular matrix modulates the hallmarks of cancer. *EMBO Rep.* **15**, 1243–1253 (2014).
13. T. Oskarsson *et al*., Breast cancer cells produce tenascin C as a metastatic niche component to colonize the lungs. *Nat. Med.* **17**, 867–874 (2011).
14. T. Oskarsson, J. Massagué, Extracellular matrix players in metastatic niches. *EMBO J.* **31**, 254–256 (2012).
15. I. Malanchi *et al*., Interactions between breast cancer stem cells and their niche govern metastatic colonization of the lung. *Nature* **481**, 85–89 (2011).
16. A. Naba *et al*., The matrisome: In silico definition and in vivo characterization by proteomics of normal and tumor extracellular matrices. *Mol. Cell. Proteomics.* **11**, M111.014647 (2012).
17. A. Naba, K. R. Clauser, J. M. Lamar, S. A. Carr, R. O. Hynes, Extracellular matrix signatures of human mammary carcinoma identify novel metastasis promoters. *eLife* **3**, e01308 (2014).
18. A. Naba *et al*., Extracellular matrix signatures of human primary metastatic colon cancers and their metastases to liver. *BMC Cancer* **14**, 518 (2014).
19. S. V. Glavey *et al*., Proteomic characterization of human multiple myeloma bone marrow extracellular matrix. *Leukemia* **31**, 2426–2434 (2017).
20. A. Naba, K. R. Clauser, D. R. Mani, S. A. Carr, R. O. Hynes, Quantitative proteomic profiling of the extracellular matrix of pancreatic islets during the angiogenic switch and insulinoma progression. *Sci. Rep.* **7**, 40495 (2017).
21. V. Gocheva *et al*., Quantitative proteomics identify Tenascin-C as a promoter of lung cancer progression and contributor to a signature prognostic of patient survival. *Proc. Natl. Acad. Sci. U.S.A.* **114**, E5625–E5634 (2017).
22. A. V. Pinho, L. Chantrill, I. Rooman, Chronic pancreatitis: A path to pancreatic cancer. *Cancer Lett.* **345**, 203–209 (2014).
23. A. Andea, F. Sarkar, V. N. Adsay, Clinicopathological correlates of pancreatic intraepithelial neoplasia: A comparative analysis of 82 cases with and 152 cases without pancreatic ductal adenocarcinoma. *Mod. Pathol.* **16**, 996–1006 (2003).
24. A. M. Tokes *et al*., Stromal matrix protein expression following preoperative systemic therapy in breast cancer. *Clin. Cancer Res.* **15**, 731–739 (2009).
25. S. Yachida *et al*., Distant metastasis occurs late during the genetic evolution of pancreatic cancer. *Nature* **467**, 1114–1117 (2010).
26. M. Saraswat *et al*., Comparative proteomic profiling of the serum differentiates pancreatic cancer from chronic pancreatitis. *Cancer Med.* **6**, 1738–1751 (2017).
27. G. Klöppel, N. V. Adsay, Chronic pancreatitis and the differential diagnosis versus pancreatic cancer. *Arch. Pathol. Lab. Med.* **133**, 382–387 (2009).
28. A. Parikh, A. F. Stephan, E. S. Tzanakakis, Regenerating proteins and their expression, regulation and signaling. *Biomol. Concepts* **3**, 57–70 (2012).
29. A. Gopinathan, J. P. Morton, D. I. Jodrell, O. J. Sansom, GEMMs as preclinical models for testing pancreatic cancer therapies. *Dis. Model. Mech.* **8**, 1185–1200 (2015).
30. S. F. Boj *et al*., Organoid models of human and mouse ductal pancreatic cancer. *Cell* **160**, 324–338 (2015).
31. T. R. Cox, J. T. Erler, Remodeling and homeostasis of the extracellular matrix: Implications for fibrotic diseases and cancer. *Dis. Model. Mech.* **4**, 165–178 (2011).
32. P. Bailey *et al*.; Australian Pancreatic Cancer Genome Initiative, Genomic analyses identify molecular subtypes of pancreatic cancer. *Nature* **531**, 47–52 (2016).
33. J. Massagué, TGFbeta in cancer. *Cell* **134**, 215–230 (2008).
34. B. Hinz, The extracellular matrix and transforming growth factor-β1: Tale of a strained relationship. *Matrix Biol.* **47**, 54–65 (2015).
35. C. Iuga *et al*., Proteomic identification of potential prognostic biomarkers in resectable pancreatic ductal adenocarcinoma. *Proteomics* **14**, 945–955 (2014).
36. D. Britton *et al*., Quantification of pancreatic cancer proteome and phosphorylome: Indicates molecular events likely contributing to cancer and activity of drug targets. *PLoS One* **9**, e90948 (2014).
37. T. Kawahara *et al*., Quantitative proteomic profiling identifies DPYSL3 as pancreatic ductal adenocarcinoma-associated molecule that regulates cell adhesion and migration by stabilization of focal adhesion complex. *PLoS One* **8**, e79654 (2013).
38. A. S. Barrett, O. Maller, M. W. Pickup, V. M. Weaver, K. C. Hansen, Compartment resolved proteomics reveals a dynamic matrisome in a biomechanically driven model of pancreatic ductal adenocarcinoma. *J. Immunol. Regener. Med.* **1**, 67–75 (2018).
39. H. F. Dvorak, Tumors: Wounds that do not heal-redux. *Cancer Immunol. Res.* **3**, 1–11 (2015).
40. C. Cyr-Depauw *et al*., Chordin-like 1 suppresses bone morphogenetic protein 4-induced breast cancer cell migration and invasion. *Mol. Cell. Biol.* **36**, 1509–1525 (2016).
41. E. L. Deer *et al*., Phenotype and genotype of pancreatic cancer cell lines. *Pancreas* **39**, 425–435 (2010).
42. R. V. Iozzo, The biology of the small leucine-rich proteoglycans. Functional network of interactive proteins. *J. Biol. Chem.* **274**, 18843–18846 (1999).
43. K. Moreth, R. V. Iozzo, L. Schaefer, Small leucine-rich proteoglycans orchestrate receptor crosstalk during inflammation. *Cell Cycle* **11**, 2084–2091 (2012).
44. X. Li *et al*., Extracellular lumican inhibits pancreatic cancer cell growth and is associated with prolonged survival after surgery. *Clin. Cancer Res.* **20**, 6529–6540 (2014).
45. X. Li *et al*., Prolonged exposure to extracellular lumican restrains pancreatic adenocarcinoma growth. *Oncogene* **36**, 5432–5438 (2017).
46. R. A. Moffitt *et al*., Virtual microdissection identifies distinct tumor- and stroma-specific subtypes of pancreatic ductal adenocarcinoma. *Nat. Genet.* **47**, 1168–1178 (2015).

47. G. Biffi *et al*., IL1-Induced JAK/STAT signaling is antagonized by TGFβ to shape CAF heterogeneity in pancreatic ductal adenocarcinoma. *Cancer Discov.* **9**, 282–301 (2019).
48. M. Awaji, R. K. Singh, Cancer-associated fibroblasts' functional heterogeneity in pancreatic ductal adenocarcinoma. *Cancers (Basel)* **11**, E290 (2019).
49. D. Öhlund *et al*., Distinct populations of inflammatory fibroblasts and myofibroblasts in pancreatic cancer. *J. Exp. Med.* **214**, 579–596 (2017).
50. R. Kalluri, The biology and function of fibroblasts in cancer. *Nat. Rev. Cancer* **16**, 582–598 (2016).
51. D. Lambrechts *et al*., Phenotype molding of stromal cells in the lung tumor microenvironment. *Nat. Med.* **24**, 1277–1289 (2018).
52. V. Bernard *et al*., Single-cell transcriptomics of pancreatic cancer precursors demonstrates epithelial and microenvironmental heterogeneity as an early event in neoplastic progression. *Clin. Cancer Res.* **25**, 2194–2205 (2019).
53. S. Nomura *et al*., FGF10/FGFR2 signal induces cell migration and invasion in pancreatic cancer. *Br. J. Cancer* **99**, 305–313 (2008).
54. H. Jiang *et al*., Targeting focal adhesion kinase renders pancreatic cancers responsive to checkpoint immunotherapy. *Nat. Med.* **22**, 851–860 (2016).
55. J. Schlessinger, Receptor tyrosine kinases: Legacy of the first two decades. *Cold Spring Harb. Perspect. Biol.* **6**, a008912 (2014).
56. S. Sigismund, D. Avanzato, L. Lanzetti, Emerging functions of the EGFR in cancer. *Mol. Oncol.* **12**, 3–20 (2018).
57. Y. Yarden, G. Pines, The ERBB network: At last, cancer therapy meets systems biology. *Nat. Rev. Cancer* **12**, 553–563 (2012).
58. M. J. Moore *et al*.; National Cancer Institute of Canada Clinical Trials Group, Erlotinib plus gemcitabine compared with gemcitabine alone in patients with advanced pancreatic cancer: A phase III trial of the National Cancer Institute of Canada Clinical Trials Group. *J. Clin. Oncol.* **25**, 1960–1966 (2007).
59. A. Naba, K. R. Clauser, R. O. Hynes, Enrichment of extracellular matrix proteins from tissues and digestion into peptides for mass spectrometry analysis. *J. Vis. Exp.*, e53057 (2015).